

Explosive site percolation and finite-size hysteresis

Nikolaos Bastas,^{*} Kosmas Kosmidis,[†] and Panos Argyrakis[‡]

Department of Physics, University of Thessaloniki, GR-54124 Thessaloniki, Greece

(Received 3 August 2011; published 15 December 2011)

We report the critical point for site percolation for the “explosive” type for two-dimensional square lattices using Monte Carlo simulations and compare it to the classical well-known percolation. We use similar algorithms as have been recently reported for bond percolation and networks. We calculate the explosive site percolation threshold as $p_c = 0.695$ and we find evidence that explosive site percolation surprisingly may belong to a different universality class than bond percolation on lattices, providing that the transitions (a) are continuous and (b) obey the conventional finite size scaling forms. Finally, we study and compare the direct and reverse processes, showing that while the reverse process is different from the direct process for finite size systems, the two cases become equivalent in the thermodynamic limit of large L .

DOI: [10.1103/PhysRevE.84.066112](https://doi.org/10.1103/PhysRevE.84.066112)

PACS number(s): 82.40.Ck, 89.75.Hc

I. INTRODUCTION

Random percolation (RP) [1–7] is a well-studied model for phase transitions in statistical physics and condensed matter physics. It consists in randomly occupying sites (site percolation) or bonds (bond percolation) on a given lattice with probability p . Neighboring occupied sites merge to form clusters. As p increases, new clusters are formed or coalesce, until at a critical value p_c , a giant component emerges, transversing the system, the well-known infinite percolating cluster.

Classical percolation and all of its variants (continuum percolation, site-bond percolation, bootstrap percolation, invasion percolation, etc. [1]), are known to be continuous transitions, exhibiting a divergent correlation length ξ at p_c . Thus, there was a stupendous surprise that recently, Achlioptas *et al.* [8] proposed a new method for the occupation of sites which produces “explosive” transitions: when filling sequentially an empty lattice with occupied sites, instead of randomly occupying a site or bond, we choose two candidates and investigate which one of them leads to the smaller clustering. The one that does this is kept as a new occupied site on the lattice, while the second one is discarded. This procedure considerably slows down the emergence of the giant component, which is now formed abruptly, thus the term explosive.

Initially, explosive percolation was considered a first-order transition [9–11]. Following these first announcements new work emerged [12,13] that doubted the above result and claimed that “explosive percolation” is actually a continuous transition with a very small β exponent [12], thus making this problem a contentious issue. Also, efforts for the establishment of a general theoretical framework for the explosive percolation have been made (e.g., [14] where the equilibrium nature of a real (discontinuous) explosive percolation process is discussed based on a Hamiltonian approach). However, a recently published paper [15] provided a rigorous mathematical proof that explosive percolation resulting from Achlioptas

processes, like the product rule, is continuous, ending the above mentioned controversy. Recently, applications of the explosive percolation transition for “real” systems have been proposed [18,19]. Up until now the systems investigated include networks and lattice bond percolation.

In this paper we extend these investigations to now include site explosive percolation and its finite-size hysteresis properties. We find that site explosive percolation indeed exhibits a very sharp transition with the β exponent “effectively” zero ($\beta/\nu \simeq 0.001$) for the case of the sum rule and $\simeq 0.04$ for the case of product rule. We investigate two variants of a reverse “Achlioptas process (AP1 and AP2)” and find that the direct and the reverse processes exhibit a hysteresis loop, which surprisingly vanishes in the thermodynamic limit.

The rest of the paper is organized as follows. In Sec. II we describe the site percolation algorithm for the direct and the reverse processes. Moreover, we describe the tools we used to examine the transition and the behavior of the system. In Sec. III we present our results and discuss their significance. Finally, in Sec. IV we sum up our main conclusions.

II. METHODS

In the present paper we use Monte Carlo simulations for the site percolation problem on an $L \times L$ square lattice with periodic boundary conditions. The algorithm for the case of the sum rule (APSR) proceeds as follows:

- (1) Initially, we start from an empty lattice. We randomly occupy one single site.
- (2) Next, we randomly select a trial unoccupied site, say A .
- (3) We calculate the size s_A of the resulting cluster to which A belongs.
- (4) We remove the trial unoccupied site A and randomly select a trial unoccupied site B , different from A .
- (5) We calculate the size s_B of the resulting cluster to which B belongs.
- (6) In case $s_A < s_B$, site A is permanently occupied and site B is discarded. In case $s_B < s_A$, site B is permanently occupied and site A is discarded. In case $s_A = s_B$, we randomly select and permanently occupy either A or B discarding the other. Each time, the number of occupied sites t is incremented by one.

^{*}nimpasta@physics.auth.gr

[†]kkosm@physics.auth.gr

[‡]panos@physics.auth.gr

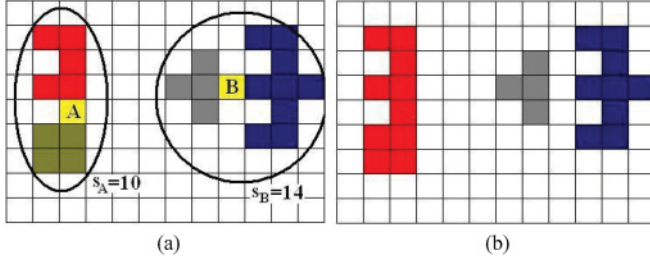


FIG. 1. (Color online) Achlioptas process according to the sum rule (APSR) for site percolation. White cells correspond to unoccupied sites while colored cells correspond to occupied sites. Different colors (red, green, gray, and blue) indicate different clusters. (a) We randomly select two trial unoccupied sites (yellow), noted by A and B , one at a time. We evaluate the size of the clusters that are formed and contain sites A and B , s_A and s_B , respectively. In this example $s_A = 10$ and $s_B = 14$. (b) According to AP, we keep site A which leads to the smaller cluster and discard site B .

(7) We repeat steps (2)–(6) until the entire lattice is covered. For each “time step” t , we monitor the size of the largest cluster S_{\max} .

In Fig. 1 we present an illustrative example of the algorithmic process, as has been previously studied. Next, we implemented the product rule (APPR). In this case, we calculate the product of the sizes of the different clusters which will merge after the placement of the new site, A or B . The only changes in the above algorithm are at steps (3) and (5). In order to compare the explosive percolation transition with the classical site percolation, using the efficient Newman-Ziff algorithm [4].

Subsequently, we simulated two variants of reverse explosive percolation processes, in order to study possible hysteresis phenomena associated with explosive percolation. We have implemented the following algorithm to simulate the reverse process AP1:

- (1) Initially, we start from a fully occupied lattice.
- (2) Next, we randomly select two trial occupied sites, say A and B . We remove them temporarily from the lattice.
- (3) Again we place one of the previous sites, say A and calculate the size s_A of the resulting cluster to which A belongs.
- (4) We go back to step (2) and repeat (3) for the case of site B , calculating the size s_B of the resulting cluster to which B belongs.
- (5) In case $s_A > s_B$, site A is reoccupied and site B is permanently discarded. In case $s_B > s_A$, site B is reoccupied and site A is permanently discarded. In case $s_A = s_B$, we randomly select and reoccupy either A or B , permanently discarding the other. Each time, the number of occupied sites t is reduced by one.
- (6) We repeat steps (2)–(5) until the entire lattice is empty. For each time step t , we monitor the size of the largest cluster S_{\max} .

In the above algorithm we did not consider periodic boundary conditions. In Fig. 2, we present an illustrative example of the algorithm used. The details are given in the figure caption. We start with a fully occupied lattice. The resulting clusters are shown in Fig. 2.

The reverse process AP2 is a slight modification of the above algorithm for AP1. At step (5) we remove the site which

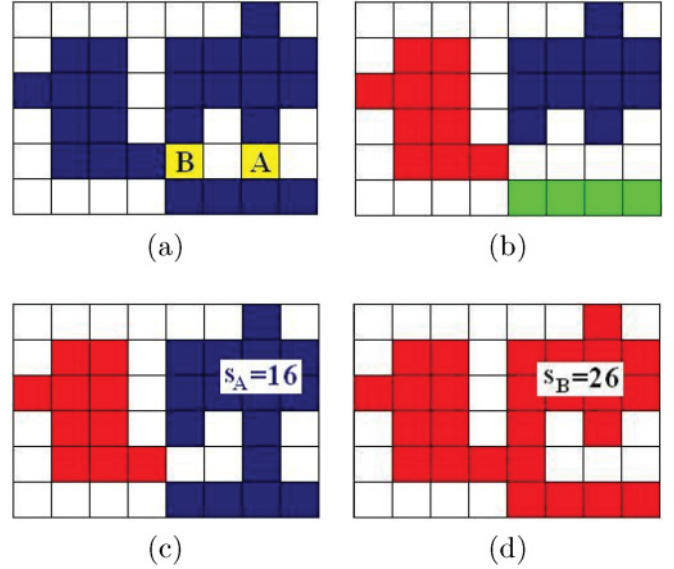


FIG. 2. (Color online) Reverse Achlioptas process (AP1) for site percolation according to the sum rule. Blue is for the occupied sites while white is for the unoccupied sites. Initially, the lattice is fully occupied. (a) An instance of the process. We randomly choose two trial sites (yellow), noted as A and B , and remove them from the lattice. (b) The clusters formed after the removal. (c) We place site A in the lattice again and calculate the size of the cluster in which it belongs, $s_A = 16$. (d) We do the same as before for the case of site B and calculate $s_B = 26$. We remove site A , which leads to the formation of the smaller cluster and keep site B .

maximizes the resulting cluster. Thus, for AP2 step (5) should be (5-AP2) In case $s_A < s_B$, site A is reoccupied and site B is permanently discarded. In case $s_B < s_A$, site B is reoccupied and site A is permanently discarded. In case $s_A = s_B$, we randomly select and reoccupy either A or B , permanently discarding the other. Each time, the number of occupied sites t is reduced by one. The rest of the algorithmic steps remain identical to AP1 described above.

Note that the main difference in the selection rule applied in the direct and in the reverse AP1 algorithm is that in the direct case, we add the site which minimizes the resulting cluster, while in the reverse AP1 case, we remove the site which minimizes the resulting cluster. Also, for clarity, we performed the opposite procedure in the reverse case [named reverse AP2 in Fig. 7(b)], i.e., we removed the sites which maximized the resulting cluster.

To track the behavior of the system, we have studied the order parameter P_{\max} defined as the ratio of the sites that belong to the largest cluster S_{\max} to the total number of sites in the lattice. For continuous transitions, P_{\max} follows the scaling relation [1,2]:

$$P_{\max} = L^{-\beta/\nu} F[(p - p_c)L^{1/\nu}] \quad (1)$$

in the vicinity of p_c . For the present analysis, we assume that the order parameter of the transition follows the conventional well-known finite size scaling. Recently, it has been suggested [13] that explosive transitions are continuous, but with an unconventional finite size scaling. We do not examine this possibility in the present paper. Moreover, we monitor the

standard deviation of the size of the largest cluster S_{\max} , defined as

$$\chi = \sqrt{\langle S_{\max}^2 \rangle - \langle S_{\max} \rangle^2}, \quad (2)$$

which has recently been proposed [11,20] as a criterion to discern between continuous and explosive transitions.

We also employed the Δ criterion proposed in [8] which quantifies the transition width of a system with size N . It is defined as $\Delta = t_1 - t_0$, where t_1 is the lowest value for which $S_{\max} > 0.5N$ and t_0 is the lowest value for which $S_{\max} > \sqrt{N}$. Achlioptas *et al.* stated that for continuous (i.e., random) percolation, this quantity should scale as $\Delta/N \rightarrow 0$ for AP and $\Delta/N \rightarrow \text{const}$ for RP as $N \rightarrow \infty$. However, this simple scaling relation does not seem to hold for bond percolation on square lattices [9].

The data given in the following figures are averages over 1000 realizations.

III. RESULTS AND DISCUSSION

In this section we present the results obtained from the calculations. In Figs. 3(a), 4(a), and 5(a) we plot the order parameter P_{\max} as a function of p , for the case of RP, APSR,

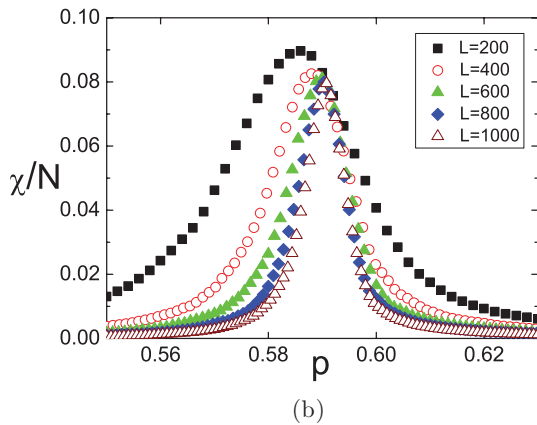
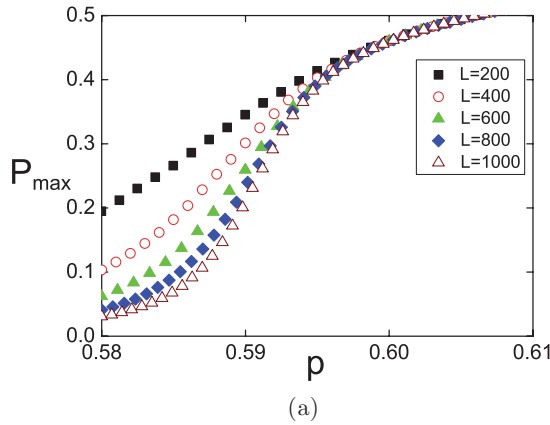


FIG. 3. (Color online) Random percolation (RP). (a) Plot of P_{\max} as a function of p for different linear sizes L . (b) Plot of χ/N as a function of p for the same sizes L as in (a). It is evident that the peaks of the curves decay as L increases. Colors are $L = 200$ (black square), $L = 400$ (open red circle), $L = 600$ (green triangle), $L = 800$ (blue diamond), and $L = 1000$ (open wine triangle).

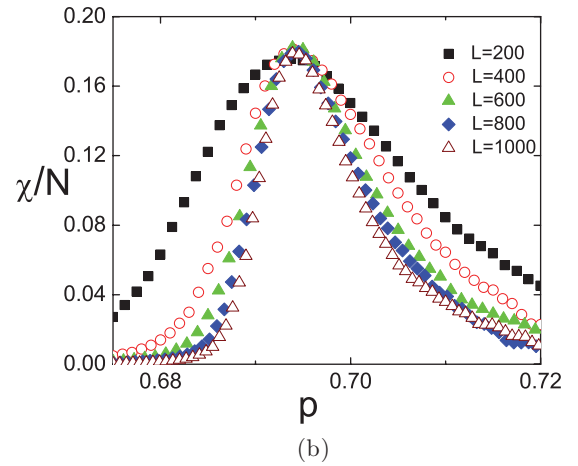
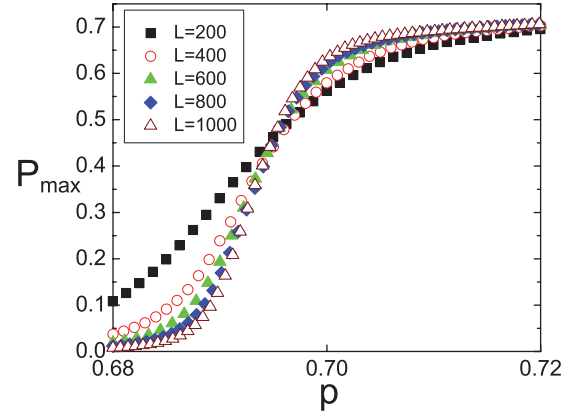


FIG. 4. (Color online) Achlioptas process with sum rule (APSR). (a) Plot of P_{\max} as a function of p for different linear sizes L for site percolation. We observe that all plotted lines pass through a single point at $p \simeq 0.695$. Moreover, we see a more abrupt jump of P_{\max} compared to Fig. 3(a). (b) Plot of χ/N as a function of p for the same sizes L as in (a). Peaks are almost constant. Colors are $L = 200$ (black square), $L = 400$ (open red circle), $L = 600$ (green triangle), $L = 800$ (blue diamond), and $L = 1000$ (open wine triangle).

and APPR models, respectively, for five different system sizes, namely, $L = 200$ (black square), $L = 400$ (open red circle), $L = 600$ (green triangle), $L = 800$ (blue diamond), and $L = 1000$ (open wine triangle). For the case of the RP model, we have recovered the correct critical exponents ($\beta/\nu \simeq 0.106$ and $1/\nu \simeq 0.75$). A comparison between Figs. 3(a), 4(a), and 5(a) shows that P_{\max} changes more abruptly in the case of AP models, as expected from an explosive transition. Moreover, in the APSR case, we observe that at $p \simeq 0.695$ all lines for the plotted system sizes seem to be crossing roughly at the same point. This p value coincides with our estimations of the transition point p_c for the APSR model, using the method of the second largest cluster as well as the value p at which the χ per lattice site (χ/N) reaches its maximum value. Using standard finite size scaling techniques, we find that $\beta/\nu \simeq 0.001$. More precisely, Eq. (1) implies that $L^{\beta/\nu} P_{\max} = F[(p - p_c)L^{1/\nu}]$ and thus, curves of $L^{\beta/\nu} P_{\max}$ vs p for different system sizes should cross at a single point at $p = p_c$. We have used our Monte Carlo

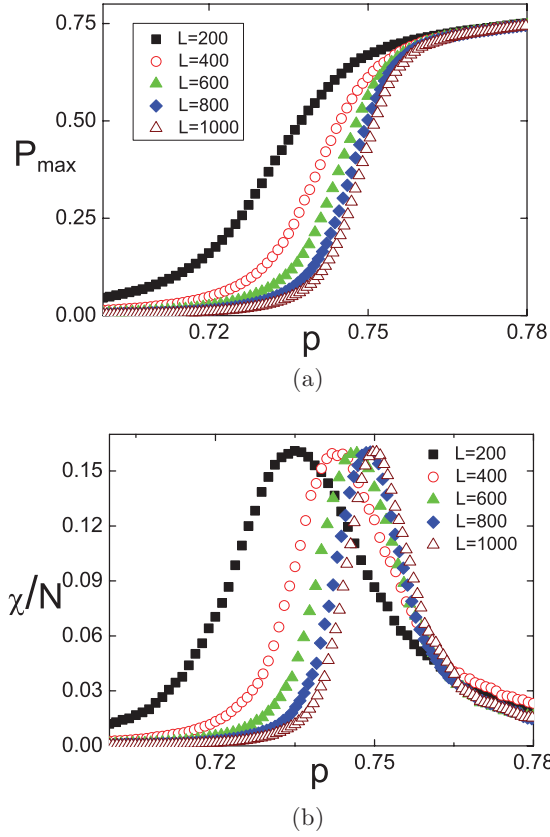


FIG. 5. (Color online) Achlioptas process with product rule (APPR). (a) Plot of P_{\max} as a function of p for different linear sizes L for site percolation. (b) Plot of χ/N as a function of p for the same sizes L as in (a). Colors are $L = 200$ (black square), $L = 400$ (open red circle), $L = 600$ (green triangle), $L = 800$ (blue diamond), and $L = 1000$ (open wine triangle).

data for P_{\max} vs p for five different sizes L , to create five functions $g_i = L^{\beta/\nu} P_{\max}$ and used minimization software to determine the values β/ν and p which minimize the sum of the squares of the pairwise differences $\Lambda \equiv \Lambda(\beta/\nu, p) = \sum_{i \neq j} (g_i - g_j)^2$.

Ideally, $\Lambda(\beta/\nu, p_c)$ should be exactly zero, but since numerical errors cannot be avoided, we consider that the values of β/ν and p that minimize Λ provide an accurate estimation of the actual values of β/ν and p_c . Such a small value for the β/ν as the one observed for the APSR, is very unusual for a continuous transition. Of course, it cannot be determined whether a transition is actually discontinuous or continuous with an extremely small β , as already discussed in Ref. [12]. It is, however, very interesting that our calculated value β/ν is different from the values calculated by Ziff [20] and Radicchi *et al.* [10] for bond percolation. They also could not reach a sharp conclusion regarding the nature of the transition. In contrast, in [12,13,16,17] numerical evidence is provided for the continuity of explosive percolation transition. Our findings indicate that in the case where the explosive transition is continuous, the site explosive percolation and bond explosive percolation belong to different universality classes. This result is both intriguing and unexpected, since in the classical case, it is well known that the critical exponents do not depend on the structure of the lattice (e.g., square or triangular) or on the

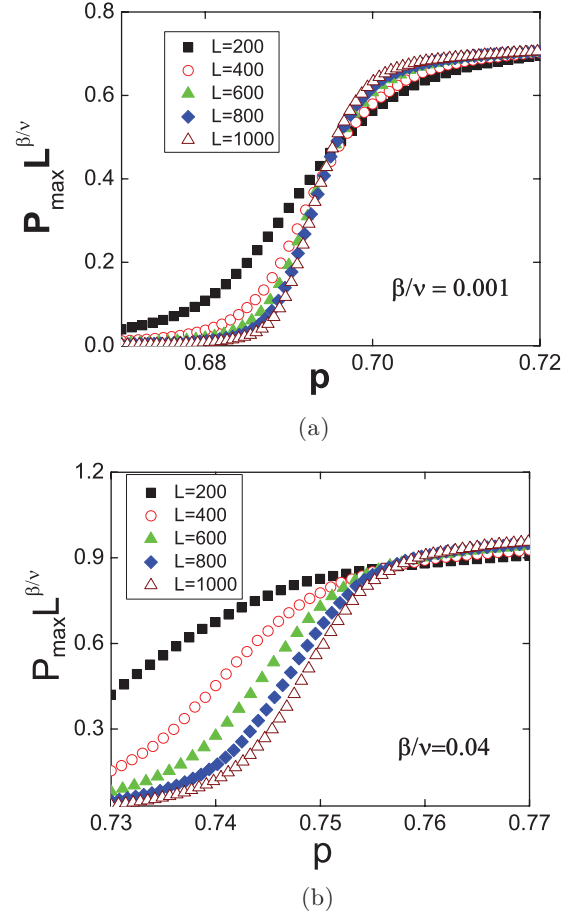


FIG. 6. (Color online) (a) Plot of $P_{\max} L^{\beta/\nu}$ as a function of p for different linear sizes L for site percolation with the sum rule. (b) Plot of $P_{\max} L^{\beta/\nu}$ as a function of p for site percolation with the product rule for the same sizes as in (a). Colors are $L = 200$ (black square), $L = 400$ (open red circle), $L = 600$ (green triangle), $L = 800$ (blue diamond), and $L = 1000$ (open wine triangle).

type of percolation (site, bond, or even continuum) [2]. We must emphasize, however, that Grassberger *et al.* [13] suggest that explosive percolation follows an unconventional finite size scaling.

In Figs. 3(b), 4(b), and 5(b), we plot the normalized standard deviation χ/N of the size of the largest cluster S_{\max} , for the same five system sizes L as above, for the RP, APSR, and APPR cases, respectively. In all cases, χ/N exhibits a sharp maximum at p_c . However, in the RP case, we observe that the maximum value is a decreasing function of L , while in the cases of APSR and APPR, it is nearly constant for large systems [see also Fig. 7(b) below for APSR].

As discussed above, Fig. 5 shows our results from the product rule simulations (APPR). Using the minimization technique previously described, we calculated the value of p_c to be $p_c = 0.756 \pm 0.006$ in accordance to [21] within error bounds. As for β/ν we calculated it to be $\beta/\nu = 0.04 \pm 0.02$. In Fig. 6, we present $P_{\max} L^{\beta/\nu}$ as a function of p both for APSR [Fig. 6(a)] and APPR [Fig. 6(b)]. In both situations, all curves cross roughly at a single point, namely, the percolation threshold p_c , as is expected from Eq. (1).

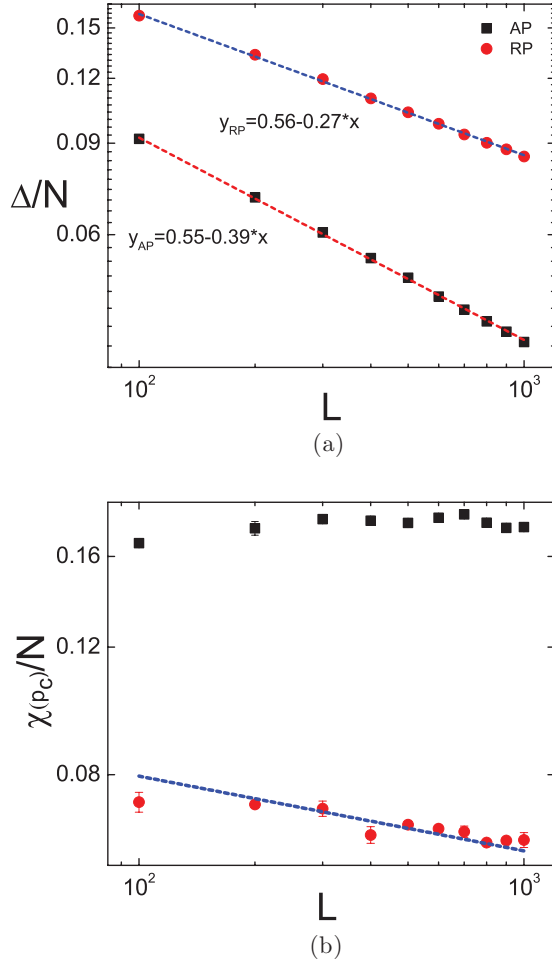


FIG. 7. (Color online) (a) Δ/N as a function of L for RP (red dots) and APSR (black squares). Both scale as a power law, with $L^{-0.27}$ for the RP case and $L^{-0.39}$ for the APSR case. (b) Plot of $\chi(p_c)/N$ as a function of L for RP (red dots) and APSR (black squares). The blue dashed line is for the theoretical prediction of the variation of $\chi(p_c)/N$ for the case of RP. We observe a power-law decay for the RP case. In the APSR case, $\chi(p_c)/N$ initially increases and reaches a plateau for large systems. Both plots are in logarithmic scale.

In Fig. 7(a), we plot the quantity Δ/N as a function of the system size L , both for RP (red dots) and APSR (black squares) models. We observe a power-law scaling for both cases, with an exponent $\omega_{RP} = -0.27$ and $\omega_{AP} = -0.39$. As expected, and in agreement with previous results reported by Achlioptas *et al.* for the case of random networks [8] and by Ziff for bond percolation on lattices [9], we find that the exponent for the AP case is much smaller than the exponent for the RP case, indicating a sharper transition for the former. Again, we observe that the exponent ω_{AP} for the site explosive percolation is different from the exponent for the case of bond explosive percolation reported by Ziff in [9], providing an additional indication that site and bond explosive percolation belong to different universality classes.

Next, we study how the quantity χ/N scales with the system size L for the classical and the explosive case. For the RP case, we expect, by a simple scaling argument, that the quantity χ/N decays as $L^{\gamma/2\nu-1}$. It is known that the variance of the order

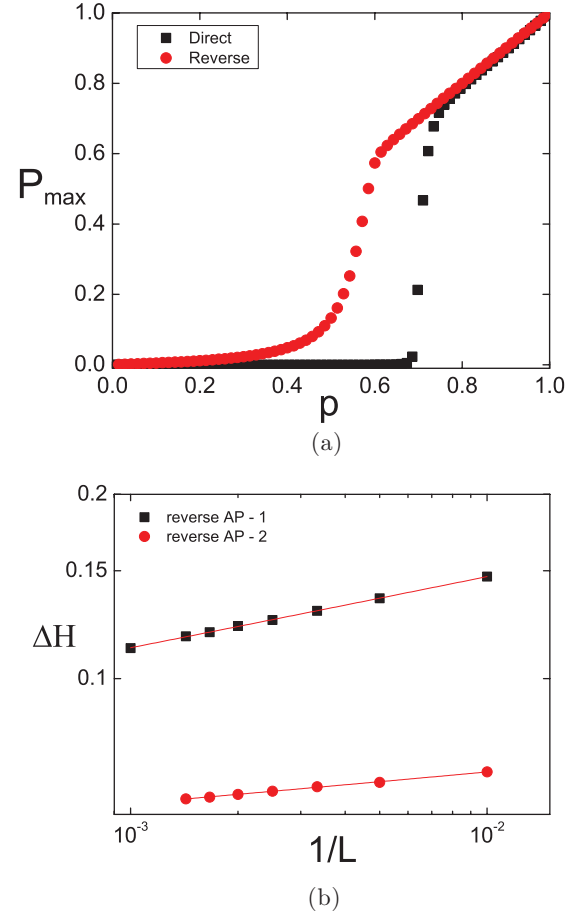


FIG. 8. (Color online) (a) Plot of the direct (black squares) and reverse (red dots) AP1 for a 700×700 lattice. The hysteresis loop is evident. (b) The area of the hysteresis loop ΔH as a function of $1/L$ (logarithmic scale). Black squares are for reverse AP1 and red dots are for reverse AP2, as described in Sec. II. For reverse AP1, $\Delta H \sim (1/L)^{0.125}$ and for reverse AP2 $\Delta H \sim (1/L)^{0.069}$. It is clear that the reverse and forward processes become equivalent in the thermodynamic limit ($L \rightarrow \infty$).

parameter P_{max} is related to the susceptibility exponent γ and scales at p_c as $\text{var}(P_{max}) \sim L^{\gamma/\nu}$. Thus, $\text{var}(S_{max}) \sim L^{\gamma/\nu+2}$. The standard deviation of the quantity S_{max} , χ , is the square root of the variance and thus, $\chi \sim L^{\gamma/2\nu+1}$. Finally, $\chi/N \sim L^{\gamma/2\nu-1}$. For the RP process, the values of γ and ν are known exactly and they are $\gamma = 43/18$ and $\nu = 4/3$. This leads to the conclusion that $\chi/N \sim -5/48 \simeq -0.1$. In Fig. 7(b), we plot $\chi(p_c)/N$ as a function of L for RP (red dots) and for APSR (black squares). Points are Monte Carlo simulation results, while the dotted line is the theoretically expected slope for the RP case. We did observe that the RP case data show a power-law decay, while for the APSR case, we observe an initial increase of χ/N followed by a plateau for large system sizes.

Finally, in Fig. 8, we present the results for the direct and the reverse AP processes (AP1 and AP2) described in Sec. II. In Fig. 8(a), we plot P_{max} as a function of p for a 700×700 lattice, both for the direct and the reverse AP1 cases. We observe that for a finite system, there exists a hysteresis loop. Of course, no such loop exists in the classical RP case,

where the process is fully reversible. We are interested in determining the scaling properties of this loop. We should emphasize that in contrast to thermal processes, we cannot associate the observed hysteresis loops with metastability and first-order transitions. We merely use the “hysteresis” concept as a means to investigate and compare different but related processes. In Fig. 8(b), we plot the area ΔH surrounded by the curves corresponding to the direct and reverse processes for various sizes L as a function of $1/L$. Black squares are for the reverse AP1 and red dots are for the reverse AP2, as described in Sec. II. The fitting suggests that $\Delta H \sim (1/L)^{0.125}$ for the former and $\Delta H \sim (1/L)^{0.069}$ for the latter. Thus, we find that, although in finite systems the reverse processes are different from the direct process, they become equivalent in the thermodynamic limit ($L \rightarrow \infty$).

IV. CONCLUSIONS

We have studied random (RP) and Achlioptas processes (APSR and APPR) for site percolation on two-dimensional square lattices. We report the critical point for the APSR as

$p_c = 0.695$ and $p_c = 0.756$ for APPR. We have shown that the order parameter P_{\max} changes more abruptly for the case of AP processes compared to the RP case. Using standard finite size scaling techniques, we find indications that explosive site and bond percolation may belong to different universality classes. A qualitatively similar behavior was also observed for Δ/N , where the exponents for explosive site and bond percolation are different. Finally, the quantity χ/N shows at p_c a power-law decay for the case of RP, while it appears to be nearly constant for large systems in the case of AP models (APSR and APPR).

We also have studied the direct and two variants of a reverse AP process. We have shown that, although in finite size systems, the reverse processes are different from the direct process, they both become equivalent in the thermodynamic limit.

ACKNOWLEDGMENTS

We thank R. Ziff and P. Grassberger for useful comments on our paper. N.B. acknowledges financial support of Public Benefit Foundation Alexander S. Onassis.

-
- [1] A. Bunde and S. Havlin, *Fractals and Disordered Systems* (Springer-Verlag, Berlin-Heidelberg, 1996).
 - [2] D. Stauffer and A. Aharony, *Introduction to Percolation Theory*, 2nd ed. (Taylor & Francis, London, 1994).
 - [3] M. E. J. Newman and R. M. Ziff, *Phys. Rev. Lett.* **85**, 4104 (2000).
 - [4] M. E. J. Newman and R. M. Ziff, *Phys. Rev. E* **64**, 016706 (2001).
 - [5] S. Kirkpatrick, *Rev. Mod. Phys.* **45**, 574 (1973).
 - [6] M. B. Isichenko, *Rev. Mod. Phys.* **64**, 961 (1992).
 - [7] J. Hoshen and R. Kopelman, *Phys. Rev. B* **14**, 3438 (1976).
 - [8] D. Achlioptas, R. M. D’Souza, and J. Spencer, *Science* **323**, 1453 (2009).
 - [9] R. M. Ziff, *Phys. Rev. Lett.* **103**, 45701 (2009).
 - [10] F. Radicchi and S. Fortunato, *Phys. Rev. E* **81**, 036110 (2010).
 - [11] N. A. M. Araújo and H. J. Herrmann, *Phys. Rev. Lett.* **105**, 035701 (2010).
 - [12] R. A. da Costa, S. N. Dorogovtsev, A. V. Goltsev, and J. F. F. Mendes, *Phys. Rev. Lett.* **105**, 255701 (2010).
 - [13] P. Grassberger, C. Christensen, G. Bizhani, S.-W. Son, and M. Paczuski, *Phys. Rev. Lett.* **106**, 225701 (2011).
 - [14] A. A. Moreira, E. A. Oliveira, S. D. S. Reis, H. J. Herrmann, and J. S. Andrade Jr., *Phys. Rev. E* **81**, 040101(R) (2010).
 - [15] O. Riordan and L. Warnke, *Science* **333**, 322 (2011).
 - [16] H. K. Lee, B. J. Kim, and H. Park, *Phys. Rev. E* **84**, 020101(R) (2011).
 - [17] J. S. Andrade Jr., H. Herrmann, A. A. Moreira, and C. L. N. Oliveira, *Phys. Rev. E* **83**, 031133 (2011).
 - [18] H. D. Rozenfeld, L. K. Gallos, and H. A. Makse, *Eur. Phys. J. B* **75**, 305 (2010).
 - [19] R. K. Pan, M. Kivelä, J. Saramäki, K. Kaski, and J. Kertész, *Phys. Rev. E* **83**, 046112 (2011).
 - [20] R. M. Ziff, *Phys. Rev. E* **82**, 051105 (2010).
 - [21] W. Choi, S.-H. Yook, and Y. Kim, *Phys. Rev. E* **84**, 020102(R) (2011).